**Abstract** Since the 1960s the minimum feature size of lithographic fabrication has shrunk from tens of micrometers to now a few nanometers, i.e. by one order of magnitude per decade. With the adaptation of lithographic techniques to the fabrication of optical elements, first micro- and more recently nanostructured optics was shown to be both feasible and useful. However, the incredibly shrinking feature size down to the scale of the optical wavelength and below does not only represent a quantitative measure, but it stands for qualitatively different optical phenomena that occur in the subwavelength regime. In that regard, micro- and nanooptics are two different worlds. Their common feature, however, is the succession of steps: computer-based design, modeling and simulation, fabrication and technology, characterization and application. We review recent progress in micro- and nanooptics by describing the state-of-the art and by emphasizing specific areas of interest.
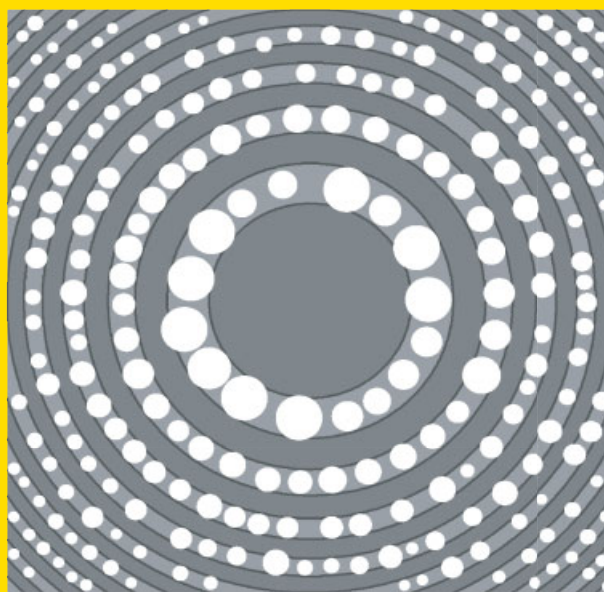
A photon sieve is a novel diffractive element which consists of many pinholes suitably arranged according to the ring pattern of a Fresnel zone plate (also shown here for instructive purposes). Position, size and density of the pinholes can be used as design parameters.

Micro- and nanooptics – an overview

Jürgen Jahns[1,], Qing Cao[1], and Stefan Sinzinger[2]*

[1] Lehrgebiet Optische Nachrichtentechnik, FernUniversität Hagen, Universitätsstr. 27, 58084 Hagen, Germany
[2] Technische Optik, Institut für Mikro- und Nanotechnologien, TU Ilmenau, Postfach 100565, 98684 Ilmenau, Germany

1. From plotters to nanoholes – a brief historical overview since the 1960s

Until the 1960s, optical technology was essentially based on the classical triad of cutting, grinding and polishing. These techniques had been invented already in ancient times: "Take 60 parts sand, 180 parts ash from sea plants, 5 parts chalk – and you get glass." [1]. Glass is still the dominant material for optics. The traditional methods for the processing of glass are grinding and polishing. Grinding is a mechanical process to remove material. The purpose of the grinding process is to obtain a surface profile that is as close as possible to the desired shape. Polishing is a mechanical as well as a chemical process. By polishing, the final shape and optical surface quality are obtained with tolerances well in the nanometer range.

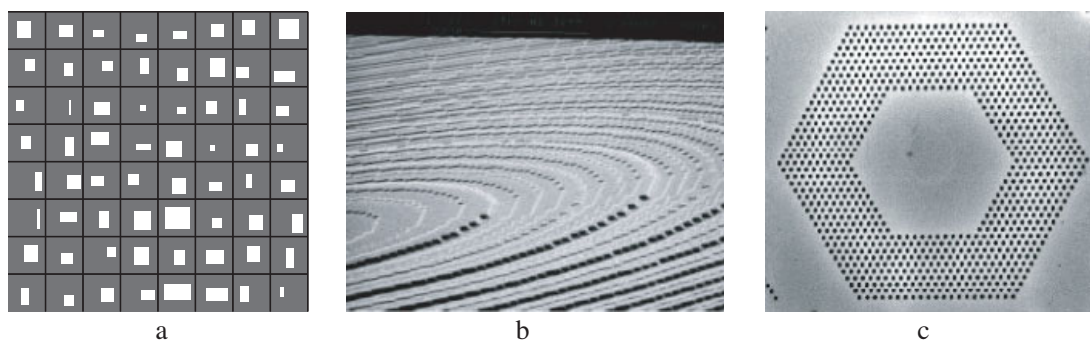Corresponding author: e-mail: jahns@fernuni-hagen.de

Figure 1 Examples for micro- and nanoscale optical elements. a) 1960: computer-generated hologram drawn by a plotter, minimum feature size $\approx 10\,\mu$m. b) 1980: diffractive element (mask lithography, 1 μm). c) 2000: photonic crystal device fabricated by electron beam lithography, resolution is 0.1 μm. (Permission granted by IEEE).

Of course, these techniques are still used today, highly optimized, and allow one to make optical elements of *macroscopic* dimensions like lenses and prisms with excellent surface quality. With the advent of computer technology, however, semiconductor processing technologies entered the stage. This has led to two implications: on the one hand, lithographic fabrication was developed as a technology for mass production, first for electronic devices. Furthermore, computers became available as powerful tools for optical design, modeling and simulation. In the meantime, lithographic techniques were adapted to the fabrication of optical and mechanical devices, first at the *micro-* and since several years at the *nanoscale* [2, 3]. The downscaling of optical devices and systems has essentially the same motivation as in electronics, namely the miniaturization and integration of elements and systems with the purpose of improving performance and reducing cost.

The terms micro- and nanooptics refer to the typical lateral feature size in an optical element. In the 1960s, the minimum feature size of lithographic fabrication was of the order of tens of micrometers. Fabrication of optical elements was often achieved by using plotters, generating huge patterns on paper or on film that were photoreduced in a subsequent step. The optical elements were called "computer-generated holograms" (Fig. 1a) and used, e.g., for analog optical signal processing [4].

An enormous push towards microoptics came in the 1980s (although the forerunners were from the 1960s and 1970s). At that time, standard lithography offered a feature size of about 1 micrometer. But, importantly, dry etching techniques were adopted to make microoptical devices like, in particular, diffractive optical elements in glass or silicon (Fig. 1b). Newly developed iterative design techniques allowed one to generate novel types of optical elements such as 1xN beamsplitters and lenslet arrays [5]. Meanwhile, microoptics is a well-established and mature technology. Microoptical components can be found in various applications, for example, as lens arrays in cameras and displays, as beam splitters and homogenizers in laser systems, as microspectrometers in analytics, etc. Recently, new potential applications like microfluidics, optical manipulation, and

biosensing, for example, have caused novel interest and generated a variety of new technological approaches.

Since around the year 2000, technology has entered the nanoscale on a broad basis: currently, electronic circuits for processors and memory chips routinely use a minimum feature size of 65 nm or less [6] (Fig. 1c). The availability of nanofabrication has stimulated research in optics and photonics tremendously. This is due to the fact that in the subwavelength regime (which happens to coincide with the nanodomain for many optical applications) nanostructures lead to new physical phenomena. Three research areas that have attracted particularly strong interest in recent years are photonic crystals, a phenomenon called enhanced transmission of light through arrays of nanoapertures in metal films, and negative-index materials.

Photonic crystals are characterized by a propagation medium with an index of refraction that is periodic with $\lambda/2$ in one, two or all three spatial dimensions [7, 8]. The term "photonic crystal" was chosen in analogy to the periodic structure of a crystal lattice. Furthermore, the periodically modulated refractive index leads to a theoretical description that is analogous to the concept of the band structure for semiconductor materials. In particular, the occurrence of a "photonic bandgap" (i.e. a range of forbidden propagation angles) is of interest to implement novel types of very compact waveguide structures, for example.

The presence of arrays of subwavelength apertures in an opaque metal film leads to a strongly enhanced transmission of light through the holes and wavelength filtering [**?**]. This effect is opening up exciting new opportunities in applications ranging from subwavelength optics and optoelectronics to chemical sensing and biophysics. The underlying physical mechanism has attracted much interest. In particular, the role of surface plasmon in the enhanced transmission is being intensively discussed.

Periodic nanostructures might exhibit unexpected properties like the phenomenon of a negative index. These materials are also known as left-handed materials [10]. The effect of a negative refractive index is associated with the simultaneous occurrence of a negative electric permittivity ε and magnetic permeability μ. It is said that this may be
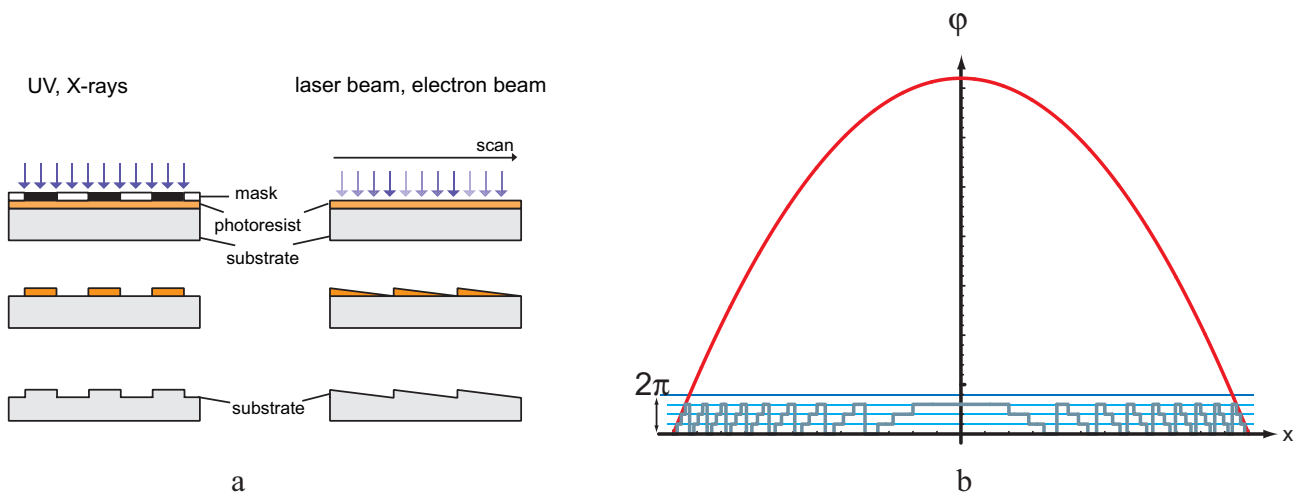
Figure 2 (online color at: www.lpr-journal.org) a) The two fundamental approaches to lithographic structuring are shown, namely mask and scanning lithography. b) shows a continuous phase profile (red curve) as is typical for refractive or reflective elements, while the quantized curve represents a diffractive element with discrete phase levels (here shown with four phase levels). Obviously, scanning (or analog) lithography is best suited for continuous profiles, while mask lithography is optimal for diffractive elements.

caused by the excitation of surface plasmon-polaritons. The inductive properties of nanoparticles may be tailored in such a way as to oppose the magnetic field of an incident light wave. As a result, an optical material consisting of an array of nanoscale electrical circuits appears to have a negative-valued μ. When coupled with a negative ε the material is expected to have a negative refractive index.

Nanostructured optical elements can also be larger than the wavelength. One example is diffractive optical elements that are used for the nanofocusing and nanoimaging of soft X-ray and EUV (extreme ultraviolet) radiation. In contrast to subwavelength nanostructured elements, we call them superwavelength nanostructured elements. Correspondingly, the related optics is called "superwavelength nanooptics." Some novel diffractive optical elements, like the photon sieve and modified Fresnel zone plates, have been suggested in the past several years for nanofocusing and nanoimaging of soft X-ray and EUV radiation and will be discussed below.

2. Microoptics

2.1. Technology and components

The most important tool for the fabrication of micro- and nanooptics is lithography, although nonlithographic techniques are of increasing interest, as we will discuss later. Lithography comprises a sequence of processing steps for structuring the surfaces of planar substrates. Two basic types of lithographic fabrication can be distinguished: mask-based lithography and scanning lithography (see, for example, [3]). In conventional mask lithography, a binary-amplitude pattern on a mask is used for the exposure of a photosensitive resist layer on a substrate (Fig. 2a). After

development the photoresist layer is structured with the mask pattern. This pattern is then transferred into the substrate, usually by some etching technique. With scanning lithography a laser or electron beam is scanned across the photoresist-coated substrate. By variation of the exposure and suitable processing it is possible to obtain a continuous surface profile in the photoresist layer. Obviously, this allows one to generate refractive elements since they have smooth continuous surfaces (red curve in Fig. 2b). In contrast, mask-based lithography is a suitable tool for making binary or multilevel diffractive elements where the geometry of the steps is important. Multilevel structures are generated by subsequent application of several mask layers. The minimum feature size depends mostly on the wavelength of the light used for the lithographic exposure.

Efficiency and design flexibility are two major characteristics of microoptical elements. Diffractive elements offer a very high degree of design flexibility, however, sometimes at the cost of relatively low efficiency. Losses are due to the phase quantization shown in the figure [11–13]. This causes unwanted diffraction orders and therefore a loss of power in the desired diffraction order. Refractive and reflective elements, on the other hand, have a high efficiency. However, usually there are limitations to functionality.

For the purpose of achieving a high efficiency, there is a strong interest in the fabrication of continuous or at least piecewise-continuous surface profiles. Thus, for microoptics fabrication, lithographic fabrication techniques have been adapted to approximate such profiles as binary multilevel structures by multimask techniques or through analog grayscale lithography. Both approaches, however, result in a significant increase in fabrication effort and cost as compared to binary optical elements and the usage of standard lithography. We will return to the issue of design flexibility and efficiency in a later section.
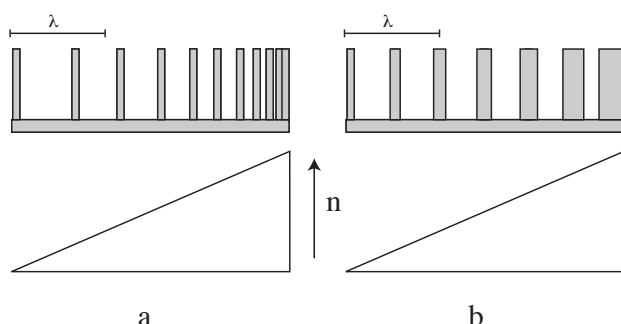
Figure 3 Implementation of blazed profiles through subwavelength structuring: a) pulse-density modulation; b) pulse-width modulation.

Since the early 1990s, the application of binary subwavelength structures for the implementation of efficient blazed micro- or nanooptical elements has become an interesting alternative to analog lithography. Continuous improvement of lithographic fabrication technology has led to standard minimum feature sizes of several tens of nanometers, i.e. well in the subwavelength range also for visible wavelengths. For periodic gratings with such feature sizes all nonzero diffraction orders become evanescent. Consequently, all the light is propagating along the direction of the zeroth diffraction order. Therefore, the name zero-order gratings has been coined for such subwavelength gratings. The effect of the subwavelength structures on the properties of the propagated wave can be conveniently understood by what is called effective medium theory. For this purpose, an "artificial refractive index" is assigned to the structured substrate that is calculated by averaging over feature sizes and depths (Fig. 3). Consequently, the refractive index of the substrate can be modulated locally by a variation of the local lithographic profiling. This allows for the fabrication of efficient blazed artificial gradient index elements. Zero-order gratings were first demonstrated for long wavelengths, i.e. water waves [14] and IR applications [15]. Later, significant improvements were suggested concerning the design, the understanding of the possible gain in diffraction efficiency with respect to conventional blazed diffraction gratings [16] as well as feasible approaches to the realization [17].

An alternative to the two standard techniques just described is holographic lithography. It has been successfully applied to the fabrication of blazed diffractive optical elements. Instead of using grayscale masks, the continuous illumination profile for photoresist exposure in this case is generated holographically, i.e. by interference of an object and a reference wavefront [18]. The use of artificially generated object wavefronts in such a configuration helps to significantly improve the bandwidth of diffractive elements fabricated with this technique [19]. Arbitrary computer-generated object wavefronts can nowadays be realized dynamically with the help of high-quality spatial light modulators such as liquid crystal on silicon (LCOS) or micromirror devices. After a spatial filtering process, which helps to achieve, e.g., precisely controlled object wavefronts that are free from higher diffraction orders, the interference pattern with the reference wavefront is used for the holographic exposure. The phase ambiguity, which in classical holography generally leads to the formation of the twin image, can be avoided by adjusting the phase values in the dynamically generated diffractive element according to specific mapping instructions. Compact illumination setups related to phase-contrast imaging have been suggested in order to minimize the problems with instabilities during the interferometric illumination process (Fig. 4) [20]. For the analog resist processing a detailed characterization of the resist properties such as e.g. absorption and bleaching, is necessary and allows a subsequent numerical simulation and optimization of the resulting profiles [21]. This very challenging task of analog photoresist processing along with the so far rather complex optical illumination setups are the main reasons why thus far in the industrial environment holographic lithography is only applied for very specific, unique solutions [22, 23].

During past years classical mechanical machining techniques for the fabrication of optical elements have been refined and optimized for the fabrication of miniature optical elements with diameters in the range of a few millimeters and have become an alternative for certain applications. This development was not only triggered by miniaturization but also by the increasing need for aspherical optical elements for optimized (macro-)optical systems. Specifically for the fabrication of aspherical optical elements precisely controlled "single point" grinding and polishing techniques
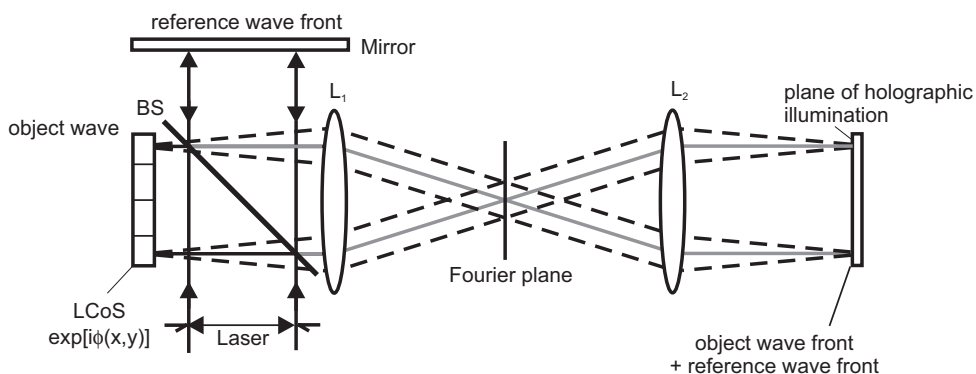

Figure 4 Schematic of a compact optical setup for holographic illumination with arbitrary computer-generated object wavefronts implemented on a liquid crystal on silicon device (LCoS). The reference wavefront is generated by the beam splitter (BS) at the entrance of the optical system and thus passes the same optical systems as the object wavefront.
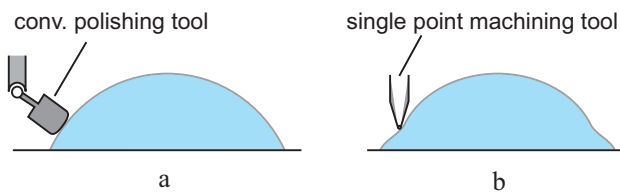
conv. polishing tool   single point machining tool

a   b

Figure 5 (online color at: www.lpr-journal.org) Schematic illustrating the difference between conventional optical polishing and single-point techniques.

have been developed. "Single point" in this case means that the mechanical ablation can be performed with high spatial resolution, thus allowing almost arbitrarily shaped profiles (Fig. 5). This represents an important technological development compared to the global mechanical treatment generally applied for fabrication of optical elements with spherical or planar surfaces. There, the optical surface quality to a large extent is a result of the statistical polishing process. In single-point fabrication processes, however, the optical precision can only be achieved with extremely high precision of the mechanical positioning system [24, 25].

Nowadays, the precision and stability of mechanical micromachining systems reaches remarkable performance. Thus techniques like "diamond turning" or "fly-cutting" have been applied for (micro-)optics fabrication already since the 1980s. In diamond turning the optical substrate is spinning at high speed and a diamond tool, which is mounted ruggedly, is then moved along precisely controlled paths. Thus, the stability of the substrate is achieved through the fast rotation so that optical surface quality with roughness in the nm range can be achieved. Single-point diamond turning is ideally suited to the fabrication of rotationally symmetric optical elements. The spectrum of profiles that can be fabricated mostly depends on the shape and diameter of the processing tools. With diamond tools of diameters as small as a few tens of micrometers even microoptical elements such as blazed diffraction gratings have been demonstrated [26]. However, the challenges for an adaptation of the technique to freeform optics remain significant since this requires additional fast and complex movements of the substrate or the tool during the fabrication process. Since these additional movements introduce additional stability problems one can consider this as a trade-off between flexibility in the achievable surface profiles and surface quality.

In fly-cutting, the substrate is mounted ruggedly while the processing tool is fixed on a spindle, which is rotating at high angular speeds and moved across the substrate for structuring. Again, since the absolute speed of the tool determines the stability of the movement, the surface quality (typical values for the surface roughness: $R_a \leq 10\,\mathrm{nm}$) in fly-cutting results from the fact that the diamond tool is mounted at a large radius off the center of rotation. In this case, however, again geometrical constraints limit the variety of surface profiles that can be processed with this approach. Fly-cutting so far has been used mostly for the
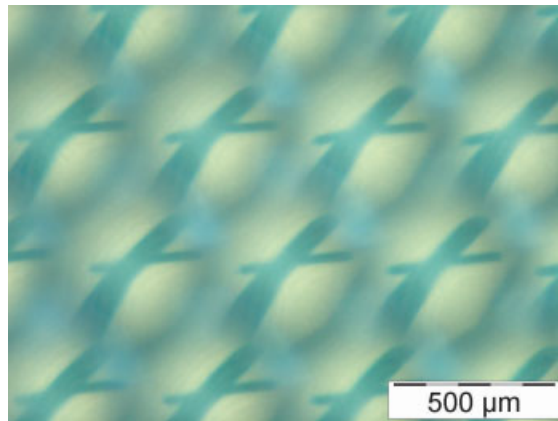

500 µm

Figure 6 (online color at: www.lpr-journal.org) Multiple images captured through a section of an array of microlenses fabricated by ultraprecision micromilling. The precision of the shape is mostly determined by the single-point diamond tool.

fabrication of metallic mirrors, e.g. for IR laser applications.

The largest flexibility in the variety of surface profiles can be achieved through ultraprecision micromilling. Systems and automatic control engineering only recently reached a state of development where one can think of using ultraprecision micromilling for optical applications. In this case, the single-point diamond tool is rotating on the rotation axis of the processing spindle. For profiling it is moved across the substrate along optimized trajectories. High rotation speed (up to 200,000 rpm), constant monitoring and control of the movement as well as optimized positioning units allow extremely precise surface profiling and surface roughness of a few tens of nm. Fig. 6 shows an array of microlenses fabricated through micromilling. Recently, ultraprecision micromilling has been successfully applied for the fabrication of a nonrotationally symmetric beam-shaping element in planar optically integrated systems [27]. In this application a peak-to-peak deviation from the desired shape of about 300 nm and a surface roughness of $R_a < 40\,\mathrm{nm}$ has been measured. Further optimization of the fabrication process is likely to result in even better quality of the elements in the near future and thus promote the field of freeform (micro-)optics. Although micromilling is not perfectly suited to the fabrication of large arrays of symmetric microoptical elements, the example illustrates the achievable optical quality. Generally, the micromilling approach will only be used for aspheric, freeform or one-dimensional cylindrical optical profiles where fabrication techniques for regular microlens arrays cannot be applied.

2.2. Microoptical systems

One of the central issues of microtechnologies, in general, is the integration of functional systems. Integrated microoptical systems are the key to real-world applications in sensing, communications and computing. It would be beyond
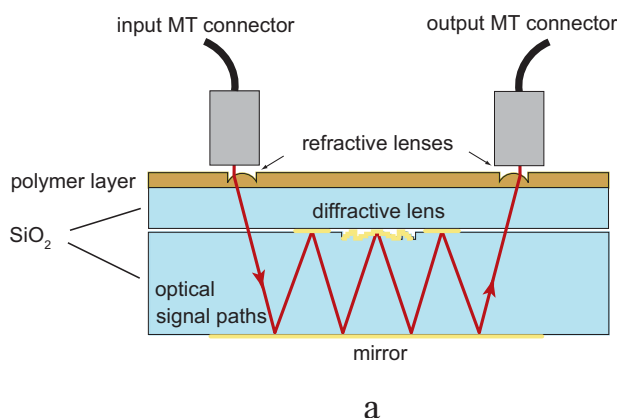
a

b

Figure 7 (online color at: www.lpr-journal.org) a) Planar-integrated microoptical system for fiber coupling combining refractive coupling elements and diffractive imaging optics. b) Replicated array of coupling lenses (after [22]).

the scope of this paper, however, to go into the details here. Instead, we consider two points that exemplify the ongoing research work. One is the optimization of the performance of optical microsystems that are used for interconnection purposes. Then, in the next section, we describe optomicrofluidics as a novel systems-oriented concept relevant for the implementation of adaptive optical solutions, for example, in biosensing.

Optical interconnection is an area of particular interest for advanced high-performance computing systems. Optics offers large temporal and spatial bandwidth. Much work has been done in this area over the past 20 years [28, 29]. Recently, the approach of silicon integrated optics has been pushed forward strongly [30], which implies that all functionality including light emission, propagation and detection are implemented in a monolithic fashion. The alternative is hybrid integration of different optical functionalities. One of the main steps that still needs to be taken with regard to systems optimization relates to the optimization of fabrication and packaging. Improved optical performance can be achieved, for example, by a combination of refractive and diffractive elements. This is particularly important for microoptical systems. We have mentioned that diffractive and reflective elements are almost complementary to each other. Refractive elements usually have a high efficiency, but their functionality is limited to simple functions such as prisms and lenses. On the other hand, diffractive elements allow one a high design flexibility, but their efficiency may sometimes be low. This suggests the following design approach: the use of refractive elements for simple functionality but high efficiency, for example, for coupling, and the use of diffractive optics where specific functionality is required (e.g., beam splitting, wavefront correction). Recently, an integrated microoptical system was built and demonstrated based on this design concept [31]. It implements an optical interconnect between two MT-fiber connectors (Fig. 7a). (Remark: The MT connector is a multifiber connector housing up to 24 fibers in a single ferrule.) In particular, the combined use of binary and analog lithography was demonstrated. A grayscale mask was generated by e-beam exposure of a HEBS (high-energy beam sensitive) glass mask with a variable shape beam e-beam writer. Contact lithography was carried out by using a special resist (Clariant

AZ4562). The resist has to have a certain thickness so that continuous profiles can be generated. Here, a resist thickness of about 50 µm was used. The lenses were then replicated into a thin layer of ORMOCER® [32]. Fig. 7b shows a section of a replicated array of refractive microlenses, each optimized for a specific coupling angle. An insertion loss of approximately 4.5 dB was demonstrated for coupling the light from one connector to the other.

2.3. Microopto fluidics

Recently, the combination of microfluidic systems with microoptical functionality has triggered a large amount of interest [33]. The reasons for this are two-fold and can be found in the potential applications of the resulting optofluidic systems. Firstly, the control of a liquid in appropriately designed optical microsystems can be applied for the control of the optical properties of the system. The second aspect promoting optofluidic systems relates to the integration of optical functionality in microfluidic systems, e.g. for biomedical applications [34–36].

Active or adaptive (micro-) optical systems often rely on the reconfigurable behavior of liquid or semiliquid material. The most prominent examples for this are liquid crystal devices, which are applied in mass products for display purposes and have been applied in adaptive optical elements. Liquid crystals consist of long chain-like molecules in a liquid environment. Upon application of an electric field a properly designed liquid crystal cell changes its optical properties, i.e. the effect on the polarization or the refractive index. This allows one to build either variable absorber cells or variable-phase elements such as lenses, prisms or even phase gratings like computer-generated holograms. So-called modal lenses or prisms that allow the implementation of continuous, i.e. nonpixelated phase functions by addressing the liquid crystal cells with a high-frequency electric field have been demonstrated [37] and successfully applied in adaptive optical systems, e.g. for astronomy [38] as well as in integrated planar optical systems [39].

Other examples of adaptive optofluidic systems are active microlenses controlled electronically, e.g. through a variation of the pressure inside the microfluidic system,
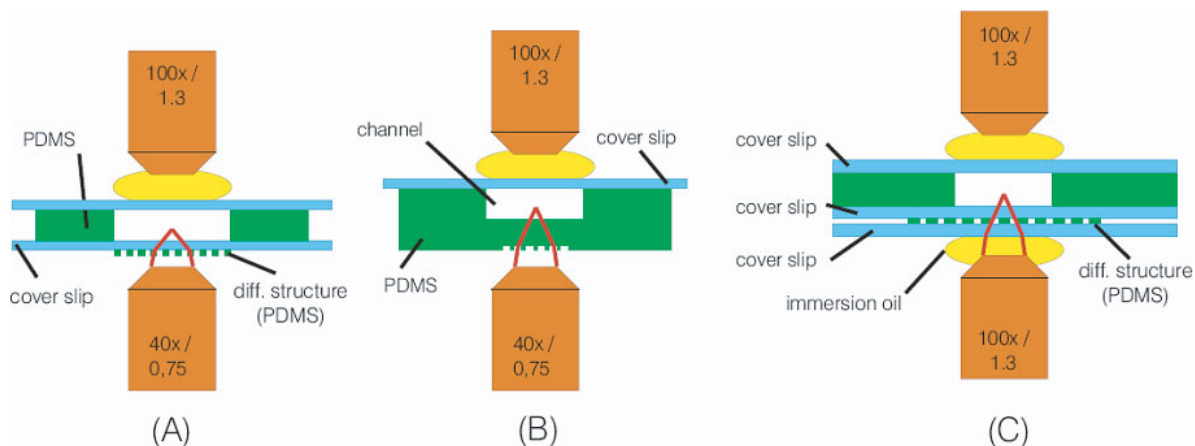
Figure 8 (online color at: www.lpr-journal.org) Concepts for the integration of optical functionality in microfluidic systems for a precise definition of the interfaces.

which changes the form of a (micro-)optical element fabricated on a flexible substrate [40,41] or through the concept of electrowetting, where the surface tension of a lens-forming liquid is varied through the application of an electric field [42,43]. Another example for adaptive optofluidic elements are optical filters based on micro- and nanostructured gratings that are filled with varying liquids, e.g. for wavelength tuning of distributed feedback lasers [44].

The integration aspect of optofluidic systems is of specific interest for applications in life science such as biomedicine or bioanalytics [45]. For these applications microfluidic systems are of specific interest since they can be designed to provide small highly efficient reaction chambers for cell or germ breeding or drug testing [46,47]. It is generally necessary to use optical techniques for analytical purposes or in more sophisticated applications for optical trapping and micromanipulation [48]. The efficient integration of optical functionality directly into in the microfluidic channel systems, e.g. through soft lithography (i.e. the replication of microoptical surface profiles into soft materials like PDMS (polydimethylsiloxane) often used for microfluidic channel fabrication) is an efficient approach towards the definition of the interface between the fluidic and the optical systems (Fig. 8) [49].

The potential of the optofluidic integration concept has been demonstrated in [50] where a highly integrated optofluidic microscope was fabricated on a chip. In principle, an ultracompact scanning microscope was implemented where the liquid flow through the microfluidic channel provides automatic scanning. High spatial resolution is achieved by the application of an array of pinholes and a corresponding detector array.

2.4. Microoptics for ultrashort pulse technology

Optical short-pulse technology using pico-/femtosecond (ps/fs) pulses is of increasing interest for communications

and processing of information as well as materials processing [51]. The handling of ultrashort pulses requires different tasks such as beam shaping, splitting and filtering in the time domain, for which microoptics can offer many interesting solutions. A specific approach to filtering is based on the use of tapped delay line filters. A tapped delay line splits an incoming signal into N branches that are delayed relative to each other and weighted differently, in general. The time delay of the nth branch relative to the first is usually $n\tau$. Two different areas of application can be envisioned depending on whether τ is smaller than the duration τ_p of the optical pulse or if $\tau > \tau_p$. In the first case, one can implement a linear filter by giving a different weight to the different facets of the array. In the second case, one can use the array, for example, as a temporal beamsplitter generating separated output pulses. For a pulse duration of typically $\tau_p = 100$ fs, the time delays that need to be generated lie in the range of 10–1000 fs. Since in free-space, the speed of light is $c = 3 \times 10^{14}$ µm/s, one needs optical structures with depth dimension in the range from 3–300 µm. These are microoptical dimensions that may, however, sometimes require rather deep profiles. Profiles with several hundreds of micrometers of depth can be generated by deep etching in silicon, by the LIGA process or by ultraprecision micromachining.

Here, we show as an example a simple implementation of a tapped delay-line using a retroreflector array. The array was cut into a block of aluminum with a pitch of $p = 640$ µm. The operation as a tapped delay line was suggested in [52] is shown in Fig. 9. By rotating the array slightly around its axis, a time delay occurs between the beamlets reflected from neighboring facets. The delay τ is determined by the rotation angle α according to $c\tau = 2p\sin(\alpha)$. The maximum number of pulses that can be generated depends on the practical implementation of the setup. The use of the tapped delay-line as a filter was shown in [52], its use as a temporal beamsplitter was demonstrated in [53]. An interesting feature is that the microoptical device is simple and compact and used in reflection. The latter
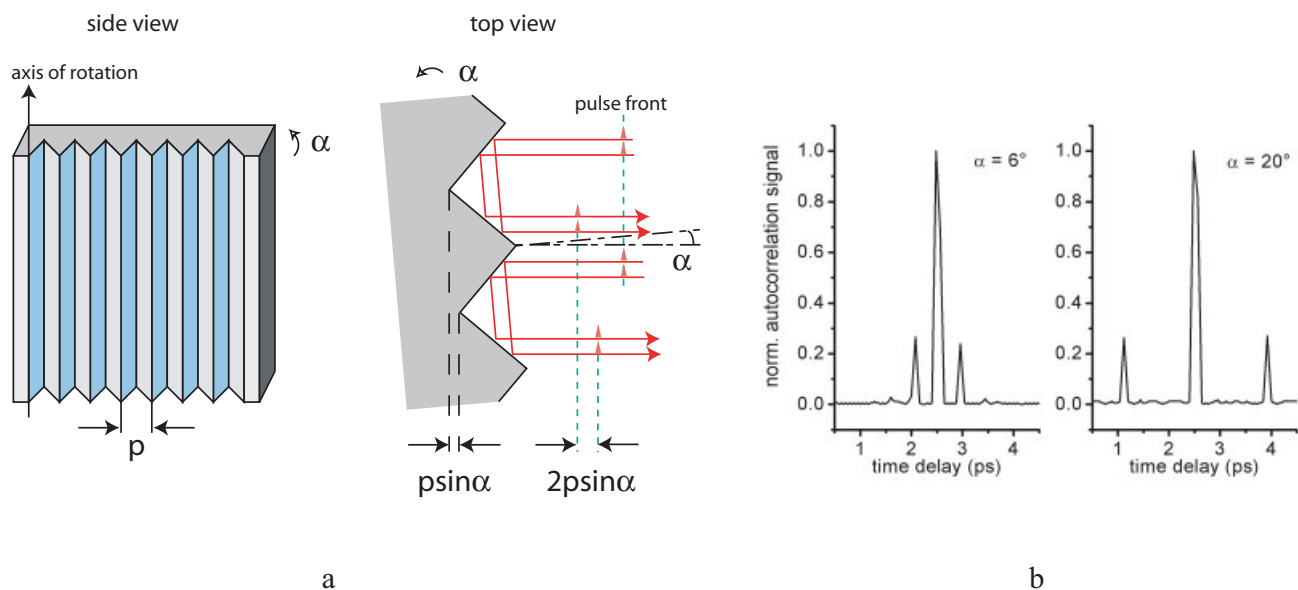
Figure 9 (online color at: www.lpr-journal.org) a) Retroreflector array as a basic element in an optical tapped delay-line for ultrashort optical pulses. A time delay between incoming pulses in two neighbouring facets when the array is slightly tilted around its axis of orientation. b) Experimental demonstration of the device as a temporal beam splitter (after [40], courtesy Optical Society of America).
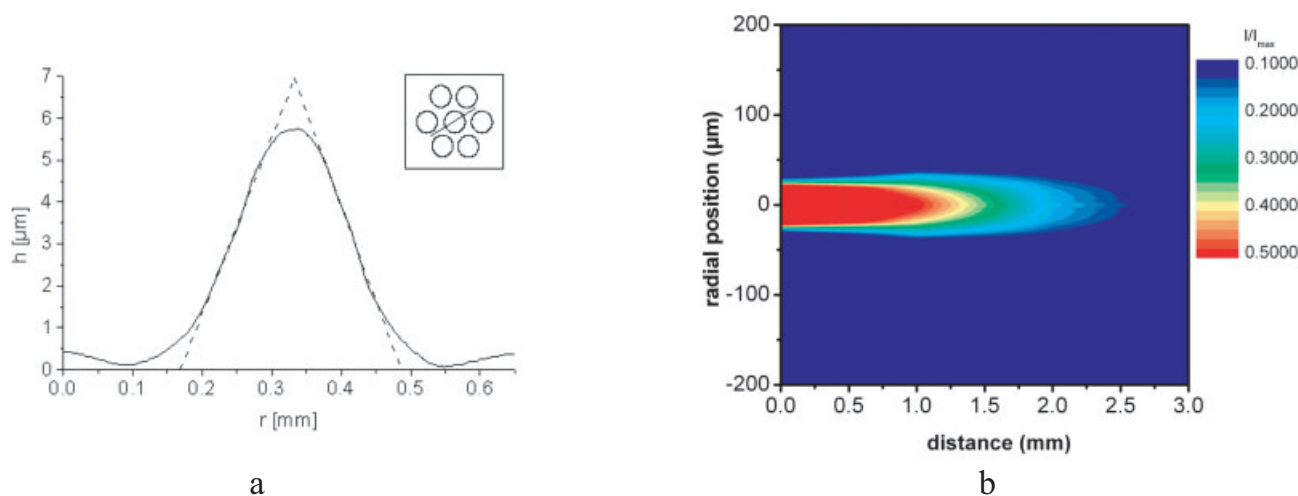

Figure 10 (online color at: www.lpr-journal.org) a) Profile of a refractive microaxicon with very shallow depth (after [42], courtesy Optical Society of America) b) Measured beam profile of the generated fs-Bessel beam (courtesy R. Grunwald).

point is of importance for fs applications in order to avoid material dispersion.

Microoptical elements can be used for the shaping of laser beams, in time and in space. Of particular theoretical and practical interest are so-called Bessel or "nondiffracting" beams. These are beams that propagate for a large distance (significantly larger than the Rayleigh distance) while keeping their lateral profile. This property may make them useful tools, for example, for the implementation of optical tweezers. An ideal Bessel beam is characterized by an amplitude profile given by the zeroth-order Bessel

function, J_0. Bessel beams can be generated by a special class of microoptical elements, the axicon. An axicon is a conical phase element with radial symmetry. The classical axicon is implemented as a refractive element. Refractive microaxicons were demonstrated by applying special thin-film deposition techniques to their fabrication [54]. Based on such elements, the generation of Bessel beams was also shown for fs pulses [55]. Fig. 10a shows the profile of a microaxicon generated by this technology and Fig. 10b shows the measured beam profile of a 10-fs Bessel beam as it propagates in the z-direction.

3. Nanooptics

As mentioned in our introduction, light can interact with nanoscale structures, regardless of subwavelength or superwavelength cases. Here, we present three examples for subwavelength nanooptics and one example of superwavelength nanooptics.

3.1. Photonic crystals

It is well known that there exist forbidden bands for electrons in periodic semiconductor materials. This kind of material is called an electronic crystal. In fact, the modern semiconductor industry is based on the concept of electronic crystals. Corresponding to electronic crystals, there also exist photonic crystals. A photonic crystal is a kind of periodic structure in which the propagation of light is forbidden for some certain frequency bands. This property can be used to confine light inside a small region, possibly even smaller than the wavelength. It has been known for a very long time that a quarter-wave stack can be used as antireflective film. In fact, a simple quarter-wave stack is a one-dimensional photonic crystal. It is said that the one-dimensional photonic crystal was first investigated by Rayleigh in 1887. One-dimensional photonic crystals have many applications ranging from Bragg mirrors, distributed feedback (DFB) lasers, and omnidirectional reflectors. In the 1970s and 1980s, various scientists began to investigate two-dimensional photonic crystals.

In 1987, Yablonovitch introduced the general concept of photonic crystals [7], especially the three-dimensional photonic crystals. Since then, photonic crystals have been attracting much interest, from both fundamental and applied researches. Extensive research works, including theoretical and experimental work has followed. A particular aspect is the simulation of these structures. Photonic crystals can be simulated by various numerical methods, such as the finite-difference time-domain (FDTD) method [56, 57], the plane-wave method, the rigorous coupled-wave method (RCWA) [58–60], and the method of lines [61, 62]. Up to now, many applications of photonic crystals have been suggested. Among them, photonic crystal waveguides and photonic crystal fibers [63–65] are extremely attractive.

One can construct a two-dimensional photonic crystal waveguide by fabricating a two-dimensional hole array in a transparent solid material. By removing certain holes, the light will be guided along the defect. This kind of waveguide is called a photonic crystal waveguide. Unlike traditional optical waveguides that use total internal reflection, photonic crystal waveguides use the bandgap effect to guide light. Because light cannot go into the region of photonic crystal, light may propagate along a subwavelength waveguide channel surrounded by the photonic crystal. Unlike a ridge waveguide, in which light is guided by total internal reflection, photonic crystal waveguides use the bandgap effect. Therefore, it is possible to create sharp bends inside a photonic crystal waveguide, disregarding here the practical difficulties with the realization of such sharp bends. It is worth mentioning that, in the third direction, i.e. in the vertical direction, light is still constrained by the traditional total internal reflection. Due to the special constraint mechanism, photonic crystal waveguides have the potential for next-generation circuits with very small dimensions.

In 1991, Russell proposed the novel idea of photonic crystal fibers [63]. Similar to photonic crystal waveguides, photonic crystal fibers also use the bandgap effect to guide light. However, unlike photonic crystal waveguides, photonic crystal fibers are uniform along the propagation direction. That is to say, the patterns at any transverse planes are the same. There are two kinds of photonic crystal fibers. One has a solid core with high refractive index in the center [64]. The other has an air hole with low refractive index in the center [65]. Light in a solid-core photonic crystal fiber is guided by both the bandgap effect and the total internal reflection. The effective index n_{eff} of a solid-core photonic crystal fiber is larger than 1 (i.e. the refractive index of air) but smaller than the refractive index of the solid material. Solid-core photonic crystal fibers were first experimentally demonstrated in 1996. Light in an air-core photonic crystal fiber is guided purely by the bandgap effect. The effective index n_{eff} of an air-core photonic crystal fiber is smaller than one. Photonic crystal fibers have special applications in many areas, such as in gas-based nonlinear optics, in atom and particle guidance, and in ultrahigh nonlinearities.

3.2. Enhanced transmission

Classical aperture theory states that the transmission through a subwavelength pinhole in metal is very low [66, 67]. Accordingly, the structure of a single pinhole in metal seems not so attractive. In 1998, it was found [68], however, that the transmission through an array of subwavelength pinholes in metal is much higher than one could expect from the transmission of a single subwavelength pinhole. This finding has attracted a lot of interest on both the physical mechanism and the applications of these structures [69–90].

In the same year of 1998, Schröter and Heitmann [71] found that the enhanced transmission can also happen for a one-dimensional subwavelength slit array in metal in the case of TM polarization. Porto, et al. [72] also simulated the enhanced transmission through a subwavelength slit array in metal. They showed that the transmittance can be more than 80 per cent of the incident energy in the near-infrared region. At that time, it was generally assumed that surface plasmons play a crucial positive role in the enhanced transmission, regardless of the two-dimensional hole array or the one-dimensional slit array. One exception is the work of Treacy [69]. He suggested that it is not the surface plasmon but dynamic diffraction that leads to the enhanced transmission, although the surface plasmon is an intrinsic part of dynamic diffraction. Cao and Lalanne [70] found and confirmed that there always appear transmission minima rather than transmission maxima when surface

plasmon resonances are most strongly excited. This surprising finding initiated a very important debate about the role of surface plasmons for enhanced transmission. Cao and Lalanne considered a subwavelength metallic grating in which the imaginary part of the relative permittivity ε can continuously change. With this kind of change, the resonant wavelength of the surface plasmon resonance also changes continuously. By using rigorous coupled wave analysis (RCWA) [91,92], Cao and Lalanne found that the transmission minima always happen at the resonant wavelengths of surface plasmon resonances. This result strongly implies that surface plasmons actually play a negative role in the enhanced transmission of one-dimensional subwavelength metallic gratings.

The nearly null transmission at the resonant wavelength of a surface plasmon has also been checked by many other authors, from both theoretical and the experimental aspects. For example, Xie et al. [73] repeated the simulation results by use of the finite-difference time-domain (FDTD) method. Pacifici et al. [74] experimentally confirmed the transmission minima at the resonances of surface plasmons.

Up to now, various enhanced transmission experiments through various materials, metallic and nonmetallic, have been reported [75]. It should be emphasized that for Cr, perfect conductors, and nonmetallic materials, there is no surface plasmon. In addition, the enhanced transmission for the TE polarization [76, 77], for which there is no surface plasmon at all, has also been reported. Quite recently [78], the enhanced transmission of acoustic waves through a subwavelength slit array was also found. For this subwavelength structure of an acoustic wave, there is also, of course, no surface plasmon. Obviously, these research works present new materials for the ongoing debate about the role of surface plasmons in the enhanced transmission.

3.3. Left-handed materials and superlenses

In nature, all materials have a positive electric permittivity ε and magnetic permeability μ. All these materials are called right-handed materials and the related electromagnetic properties can be described by Maxwell's equations. In 1968, Veselago [10] showed theoretically that Maxwell's equations can also be satisfied if the electric permittivity ε and the magnetic permeability μ are both negative at the same time. Those materials with negative electric permittivity ε and negative magnetic permeability μ are called left-handed materials. There is no left-handed material in nature. It was predicted that left-handed materials can be made by periodic metallic structures. One interesting property of left-handed materials is the so-called negative refraction: in this case, the angle of the light refracted at an interface between a right-handed material and a left-handed material is negative. The idea of the superlens [93] is based on the so-called negative refraction.

It is well known that there are two limits for the resolution of imaging. The first one comes from the diffraction limit, which is related to the numerical aperture. One may increase the resolution by increasing the numerical aperture. The second limit results from the property that evanescent waves cannot propagate to the far field. This means that one cannot get a resolution better than half of the wavelength in the far field. In 2000, Pendry [93] claimed that a superlens that is composed of left-handed material can overcome the limit due to the lacking evanescent waves. He argued that evanescent waves can be amplified by using a left-handed material. As a consequence, he claimed that one can build a "superlens" and get a perfect image. Pendry's work has attracted a lot of interest. In 2005 it was reported that the concept of the superlens was experimentally demonstrated by use of a very thin silver film [94].

3.4. Diffractive nanofocusing and imaging

Similar to *subwavelength* nanooptics, as explained in our introduction, *superwavelength* nanooptics has also made significant progress during the past decade. One important area is diffractive nanofocusing and nanoimaging of soft X-ray and extreme ultraviolet (EUV) radiation [95–105]. For focusing and imaging in the visible spectral region, one can use refractive lenses with high efficiency. In this spectral region, many transparent materials can be used to make lenses. However, in the spectral regions of soft X-rays and EUV radiation, all solid materials are strongly absorbing. As a consequence, one cannot make any refractive lens in these spectral regions. However, one can use Bragg reflectors with many alternate layers to realize focusing and imaging in these spectral regions. It was reported that Bragg reflectors with alternate dielectric and metallic layers were used in the SOHO (Solar and Heliospheric Observatory) experiment [106]. Recently, it was also reported that Bragg reflectors were used for the experiments for nanolithography in the EUV region. Another possibility is the use of diffractive optical elements. For example, traditional Fresnel zone plates can be used for the nanofocusing and nanoimaging of soft X-ray and EUV radiation [101–103]. The Fresnel zone plate was first proposed by Rayleigh in an unpublished work. The first published literature on this kind of element was written by Soret [107]. Therefore, the traditional Fresnel zone plate is also called a "Soret lens."

The traditional Fresnel zone plate has been employed successfully in soft X-ray microscopy for about 40 years. A schematic view of a soft X-ray microscope is shown in Fig. 11. A partially coherent light beam from a synchrotron radiation source is first focused by a large condenser zone plate. The focused beam, after passing a small pinhole, is used as the illuminating light beam for the sample. The illuminated sample is then imaged onto the CCD detector by a microzone plate. Usually, the magnification is about thousands of times. The resolution of a traditional Fresnel zone plate is about the order of the width of the outermost open ring. Currently, the minimum feature size that can be fabricated is about 15–40 nm. By using a zone plate with a minimum feature size of about 15 nm and the partially
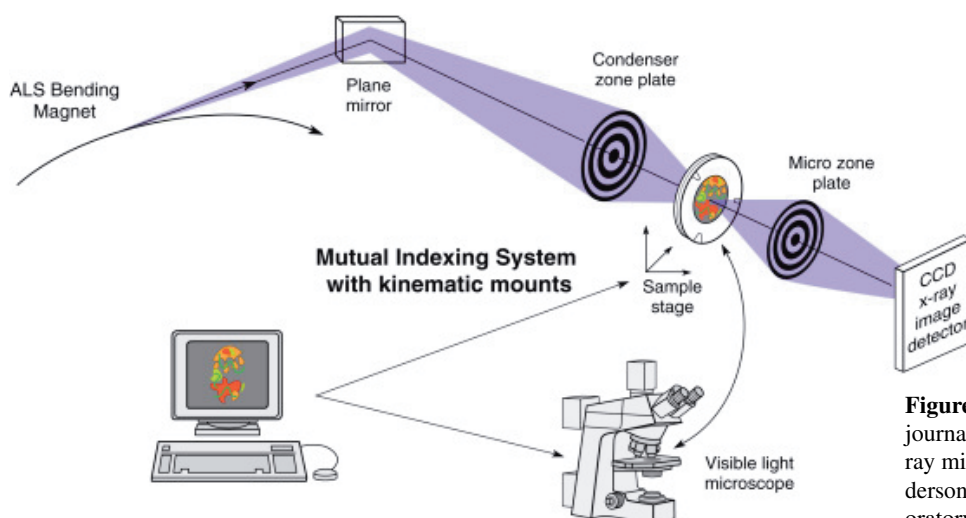
Figure 11 (online color at: www.lpr-journal.org) Schematic view of a soft X-ray microscope (courtesy of Dr. E. H. Anderson, Lawrence Berkeley National Laboratory).
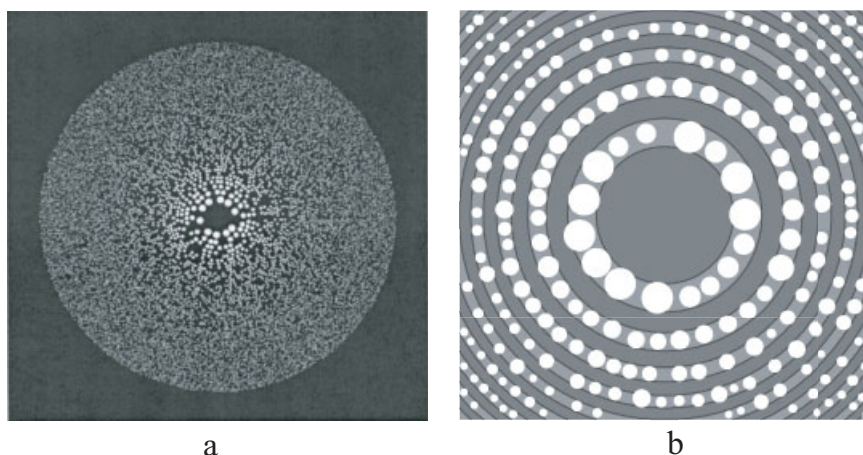

a   b

Figure 12 a) Photograph [after G. Andersen, Opt. Lett. **30**, 2976–2978 (2005)] and b) schematic view of a photon sieve. In the schematic rendering b), the positions of the pinholes are shown in front of the rings of a Fresnel zone plate. The amplitude of the light passing through a specific pinhole is given by its area, the phase by its position. Positions in front of light and dark rings differ in phase by π.

coherent illumination, Lawrence Berkeley National Laboratory has reached a resolution that is better than 15 nm [100].

To achieve higher resolution, recently, Kipp et al. [95] proposed the novel idea of the photon sieve. As shown in Fig. 12, unlike a zone plate that is composed of concentric rings, a photon sieve is composed of a great number of pinholes. Their positions and radii have to be properly chosen. By allowing the sizes of the pinholes to be larger than the sizes of the local half-zones of the underlying traditional Fresnel zone plate, a photon sieve can resolve a spot that is much smaller than the minimum feature size. This can be achieved because of an increased value of the numerical aperture (i.e. a larger total radius for a fixed focal length f). In addition, by use of a smooth filtering on the population of the pinholes, the sidelobes of the focal spot shape can also be significantly suppressed.

Cao and Jahns [96, 97] established an individual far-field model for photon sieves. This model is based on the fact that, at the focal plane, the individual diffracted fields have already reached their own far fields, even though the total diffracted field distribution has not reached the far field.

Because the far field of a circular pinhole can be analytically described by the Airy-pattern distribution, this model is simple and accurate. It can be used, on the one hand, for the focusing analysis and the design of a photon sieve, and on the other hand, for accurate and fast simulation of a photon sieve.

Cao and Jahns [98] also proposed a modified Fresnel zone plate to produce a sharp Gaussian focal spot. This kind of diffractive optical element can realize the same functions as a photon sieve. More recently, Cao and Jahns [99] further established a general theory for general modified Fresnel zone plates and the related fast simulation method. With the help of this simple and fast simulation method, Vaschenko et al. [105] have generated an ablation of only 82 nm by focusing the laser beam of a tabletop soft X-ray laser. It should be mentioned that Andersen [108] has suggested the novel photon sieve space telescope, though this work is not in the field of nanooptics (because the minimum feature size is much larger than the nanometer scale). This kind of space telescope can be as large as 20 m, which is much larger than the famous Hubble space telescope.

4. Conclusion

We have presented a review of micro- and nanooptics and showed that these are areas of active and intensive research. There is tremendous potential applying the new technologies and phenomena for many areas of application. Notable are novel approaches to classical areas of optics such as high-resolution imaging and sensing. Also of interest are new concepts like, for example, the use of microoptics for femtosecond-pulse technology as well as compact devices for integrated optical circuits and systems. There are, of course, numerous interesting areas of research that we have not been able to touch on here. Among them is the wide and rapidly growing field where the "mechanical properties" of light are exploited, for example, in the manipulation of particles by optical tweezers and optical traps [109, 110] or in the context of the orbital angular momentum [111, 112]. With regards to the aspect of optical fabrication and technology, an area too big to be included here is the field of gradient-index optics and its applications [113–115]. The interested reader is referred to the literature for also finding out about those areas.

Jürgen Jahns was born in Erlangen, Germany, in 1953. He received the diploma and doctorate in physics from the University of Erlangen-Nürnberg, Germany, in 1978 and 1982, respectively. From 1983 to 1986, he was with Siemens AG, Munich, Germany, where he worked on robotics, sensors, and optical fiber communications. From 1986 to 1994, he was a Member of the Technical Staff in the Optical Computing Research Department, AT&T Bell Laboratories, Holmdel, NJ. During that time, he worked on optical interconnections, diffractive optics, and microoptic systems integration. Since 1994, he has been a Full Professor and Chair of Optical Information Technology at the Fernuniversität Hagen, Germany. With his group he is currently working on microoptics and nanooptics for short pulses and interconnection. Jürgen Jahns has (co-)authored more than 80 journal articles and several textbooks on photonics and microoptics. He is a member of the German Society for Applied Optics (DGaO), the European Optical Society (EOS) and the Institute of Electrical and Electronic Engineers (IEEE), he became Fellow of the Optical Society of America (OSA) in 1998 and of the International Society of Optical Engineering (SPIE) in 2007.

Qing Cao received his B. S. degree in physics from Zhejiang University, China, in 1989, his Ph. D degree in optics from the Chinese Academy of Sciences in 1994, and his Habilitation degree in photonics from Fernuniversität Hagen, Germany, in 2007. He worked with the Chinese Academy of Sciences, CNRS of France, and Fernuniversität Hagen for many years. His representative scientific contributions include the finding of transmission minimum of subwavelength metallic gratings at surface plasmon resonances, the first analytical model for photon sieve and the general theory (including simulation method) for modified Fresnel zone plates, and the first theoretical explanation for metal wire terahertz waveguide. Qing Cao is the first author of nearly 40 journal articles in the field of optics. He has received more than 371 scientific citations (SCI). In particular, the paper published in Physical Review Letters 88, 057403 (2002) has been cited more than 138 times (SCI). Qing Cao is a reviewer for many international scientific journals.

Stefan Sinzinger received his Dipl.-Phys. and Dr. rer. nat. degrees from the Friedrich-Alexander Universität (FAU) Erlangen-Nürnberg (Germany), Institute for Applied Optics (Prof. Dr. A. W. Lohmann), in 1989 and 1993, respectively. In 1990/1991 he spent 9 months at the NEC Research Center performing research on computer holography. In 1994 he joined Prof. Dr. J. Jahns at the Institute for Information Technology (Optische Nachrichtentechnik) at the Fernuniversität Hagen, Germany, where he was performing research on planar microoptical systems integration. In 2002, he was appointed Chair of the department for "Technische Optik" (Optical Engineering) at the Technische Universität Ilmenau, Fakultät für Maschinenbau (Mechanical Engineering Department). He serves as a reviewer for various international optical journals and is an Associate Editor of the SPIE "Journal of Micro/Nanolithography, MEMS and MOEMS". He has (co-)authored numerous journal articles and a standard textbook on microoptics. His current research is focused on design, fabrication and integration of microoptical elements and hybrid optofluidic microsystems, optical tweezing as well as on ultraprecision machining for optical microsystems.

References

[1] H. Bach and N. Neuroth (eds.), The Properties of Optical Glass (Springer, Berlin, 1995).

[2] H.-P. Herzig (ed.), Micro-optics: Elements, Systems, and Spplications (Taylor & Francis, London, 1997).

[3] S. Sinzinger and J. Jahns, Microoptics, 2nd ed. (Wiley-VCH, Weinheim, 2003).

[4] B. R. Brown and A. W. Lohmann, Complex spatial filtering with binary masks, Appl. Opt. **5**, 967–969 (1966).

[5] T. J. McHugh and W. B. Veldkamp, Binary optics, Sci. Am. **266**, 92–97 (1992).

[6] J. K. Hwang, H. Y. Ryu, D. S. Song, I. Y. Han, H. K. Park, D. H. Jang, and Y. H. Lee, Continuous room-temperature operation of optically pumped two-dimensional photonic crystal lasers at 1.6 μm, IEEE Photon. Technol. Lett. **12**, 1295–1297 (2000).

[7] E. Yablonovitch, Inhibited spontaneous emission in solid state physics and electronics, Phys. Rev. Lett. **58**, 2059–2062 (1987).

[8] J. Joannopoulos, R. D. Meade, and J. N. Winn, Photonic Crystals – Molding the Flow of Light (Princeton University Press, Princeton, 1995).

[9] T. W. Ebbesen, H. J. Lezec, H. F. Ghaemi, T. Thio, and P. A. Wolff, Extraordinary optical transmission through sub-wavelength hole arrays, Nature **391**, 667–669 (1998).

[10] V. G. Veselago, The electrodynamics of substances with simultaneously negative values of ε and μ, Sov. Phys. Usp. **10**, 509–514 (1967).

[11] J. W. Goodmann and A. M. Silvestri, Some effects of Fourier-domain phase quantization, IBM J. Res. Dev. **14**, 478– (1969).

[12] W. J. Dallas, Phase quantization – a compact derivation, Appl. Opt. **10**, 673–674 (1971).

[13] W. J. Dallas, Phase quantization – a few illustrations, Appl. Opt. **10**, 674 (1971).

[14] W. Stork, N. Streibl, H. Haidner, and P. Kipfer, Artificial distributed-index media fabricated by zero-order gratings, Opt. Lett. **16**, 1921–1923 (1991).

[15] H. Haidner, P. Kipfer, J. T. Sheridan, J. Schwider, N. Streibl, M. Collischon, J. Hutfless, and M. Marz, Diffraction grating with rectangular grooves exceeding 80% diffraction efficiency, Infrared Phys. **34**, 467–475 (1993).

[16] P. Lalanne, S. Astilean, P. Chavel, E. Cambril, and H. Launois, Design and fabrication of blazed binary diffractive elements with sampling periods smaller than the structural cutoff, J. Opt. Soc. Am. A **16**, 1143–1156 (1999).

[17] B. H. Kleemann, J. Ruoff, and R. Arnold, Area-coded effective medium structures, a new type of grating design, Opt. Lett. **30**, 1617–1619 (2005).

[18] R. C. Fairchild and J. R. Fienup, Computer originated hologram lenses, Opt. Eng. **21**, 133–140 (1982).

[19] H. Bartelt and S. K. Case, High-efficiency hybrid computer generated holograms, Appl. Opt. **21**, 2886–2890 (1982).

[20] M. Teschke and S. Sinzinger, Modified phase contrast for the recording of holographic optical elements, Opt. Lett. **32**, 2067–2069 (2007).

[21] M. Hofmann, S. Leopold, S. Stoebenau, M. Burkhardt, R. Brunner, and S. Sinzinger, Photoresist characterization for analog lithography in the visible range, submitted to Opt. Eng.

[22] C. J. M. van Rijn, Laser interference as a lithographic nanopatterning tool, J. Microlithogr. Microfabr. Microsyst. **5**, 011012 (2007).

[23] M. Burkhardt and R. Brunner, Functional integrated optical elements for beam shaping with coherence scrambling properties realized by interference lithography, Appl. Opt. **46**, 7061–7067 (2007).

[24] E. Brinksmeier and O. Riemer, Wirkmechanismen bei der Mikrozerspanung, Mater.wiss. Werkst.tech. **31**, 754–759 (2000).

[25] A. Katz and L. Kugler, Hochpräzise Maschinenkonzepte zur Bearbeitung harter Werkstücke durch Mikroschleifen (in German), in: Jahrbuch Schleifen, Honen, Läppen und Polieren, 62. Aufl., (Vulkan Verlag, Essen, 2005).

[26] G. C. Blough, M. Rossi, A. K. Mack, and R. L. Michaelis, Single-point diamond turning and replication of visible and near infrared diffractive optical elements, Appl. Opt. **36**, 4648–4654 (1997).

[27] S. Stoebenau, M. Amberg, and S. Sinzinger, Ultraprecision micromilling of freeform optical elements for planar microoptical systems integration, in: Proceedings of the SPIE Photonics Europe 2008.

[28] J. W. Goodman, F. J. Leonberger, S.-Y. Kung, and R. Athale, Optical interconnections for VLSI, Proc. IEEE **72**, 850–866 (1984).

[29] J. Jahns, Free-space optical computing and interconnection, in: Progress in Optics XXXVIII, edited by Emil Wolf (North-Holland, Amsterdam, 1998).

[30] G. T. Reed, The optical age of silicon, Nature **427**, 595–596 (2004).

[31] R. Heming, L.-C. Wittig, P. Dannberg, M. Gruber, J. Jahns, and E.-B. Kley, Efficient planar-integrated free-space optical interconnects fabricated by a combination of binary and analog lithography, to be published in J. Lightwave Technol. (2008).

[32] R. Buestrich, F. Kahlenberg, M. Popall, P. Dannberg, R. Müller-Fiedler, and O. Rösch, ORMOCER®s for optical interconnection technology, J. Sol-Gel Sci. Technol. **20**, 181–186 (2001).

[33] D. Psaltis, S. R. Quake, and C. Yang, Developing optofluidic technology through the fusion of microfluidics and optics, Nature **442**, 381–386 (2006).

[34] M. L. Chabinyc, D. T. Chiu, J. C. McDonald, A. D. Stroock, J. F. Christian, A. M. Karger, and G. M. Whitesides, An integrated fluorescence detection system in poly(dimethylsiloxane) for microfluidic applications, Anal. Chem. **73**, 4491–4498 (2001).

[35] K. B. Mogensen, Y. C. Kwok, J. C. Eijkel, N. J. Petersen, A. Manz, and J. P. Kutter, A microfluidic device with an integrated waveguide beam splitter for velocity measurements of flowing particles by Fourier transformation, Anal. Chem. **75**, 4931–4936 (2003).

[36] E. Verpoorte, Chip version-optics for microchips, Lab Chip **3**, 42N–52N (2003).

[37] A. F. Naumov, M. Y. Koktev, I. R. Guralnik, and G. V. Vdovin, Liquid crystal adaptive lenses with modal control, Opt. Lett. **23**, 992–998 (1998).

[38] A. F. Naumov, G. D. Love, M. Yu. Loktev, and F. L. Vladimirov, Control optimization of spherical modal liquid crystal lenses, Opt. Exp. **4**, 344–352 (1999).

[39] M. Amberg and S. Sinzinger, Design considerations for efficient planar optical systems, Opt. Commun. **267**, 74–78 (2006).

[40] J. Chen, W. Wang, J. Fang, and K. Varahramyan, Variable focusing microlens with microfluidic chip, Micromech. Microeng. **14**, 675–680 (2004).

[41] A. Werber and H. Zappe, Tunable microfluidic microlenses, Appl. Opt. **44**, 3238–3245 (2005).

[42] M. Vallet, M. Vallade, and B. Bergé, Limiting phenomena for the spreading of water on polymer films by electrowetting, Eur. Phys. J. B **11**, 583–591 (1999).

[43] B. Bergé and J. Peseaux, Variable focus lens controlled by an external voltage: an application to electrowetting, Eur. Phys. J. E **3**, 159–163 (2000).

[44] L. Diehl, B. G. Lee, P. Behroozi, M. Loncar, M. Belkin, F. Capasso, T. Aellen, D. Hofstetter, M. Beck, and J. Faist, Microfluidic tuning of distributed feedback quantum cascade lasers, Opt. Exp. **14**, 11667 (2006).

[45] J. Jahns and S. Sinzinger, Microoptics for biomedical applications, Am. Biotechnol. Lab. **11**, 52–54 (2000).

[46] K. Martin, Th. Henkel, V. Baier, A. Grodrian, Th. Schön, M. Roth, J. M. Köhler, and J. Metze, Generation of large number of separated microbial populations by cultivation in segmented-flow microdevices, Lab Chip **3**, 202–207 (2003).

[47] A. Grodrian, J. Metze, Th. Henkel, K. Martin, M. Roth, and J. M. Köhler, Segmented flow generation by chip reactors for highly parallelized cell cultivation, Biosens. Bioelectron. **19**, 1421–1428 (2004).

[48] K. Ramser, J. Enger, M. Goksör, D. Hanstorp, K. Logg, and M. Käll, A microfluidic system enabling Raman measurements of the oxygenation cycle in single optically trapped red blood cells, Lab Chip **5**, (2005).

[49] S. Sinzinger, M. Amberg, A. Oeder, and D. Hein, Integrated micro-opto-fluidic systems for optical manipulation of cell cultures, in: Frontiers in Optics, OSA Technical Digest (CD) (Optical Society of America, Washington, D. C., 2007), paper FWH4.

[50] X. Heng, D. Erickson, L. R. Baugh, Z. Yaqoob, P. W. Sternberg, D. Psaltis, and C. Yang, Optofluidic microscopy - a method for implementing a high-resolution optical microscope on a chip, Lab Chip **6**, 1274–1276 (2006).

[51] J. C. Diels and W. Rudolph, Ultrashort laser pulse phenomena, 2nd ed. (Academic Press, Burlington, 2006)

[52] A. Sabatyan and J. Jahns, Retroreflector array as tapped delay-line filter for ultra-short optical pulses, J. Eur. Opt. Soc. RP **1**, 06022 (2006).

[53] R. Grunwald, M. Bock, and J. Jahns, Femtosecond-laser pulse shaping with microoptical retroreflector arrays, Conf. Lasers and Electro-Optics, paper CTuU3 (2008).

[54] R. Grunwald, Thin Film Micro-optics (Elsevier, Amsterdam, 2007).

[55] R. Grunwald, U. Griebner, F. Tschirschwitz, E. T. J. Nibbering, T. Elsaesser, V. Kebbel, H.-J. Hartmann, and W. Jüptner, Generation of femtosecond Bessel beams with microaxicon arrays, Opt. Lett. **25**, 981–983 (2000).

[56] K. S. Yee, Numerical solution of initial boundary value problems involving Maxwell's equations in isotropic media, IEEE Trans. Antennas Propag. **14**, 302–307 (1966).

[57] A. Taflove and S. C. Hagness, Computational Electrodynamics: The Finite-difference Time-domain Method, 2nd ed. (Artech House, Boston, 2000).

[58] Ph. Lalanne and E. Silberstein, Fourier-modal methods applied to waveguide computational problems, Opt. Lett. **25**, 1092–1094 (2000).

[59] E. Silberstein, Ph. Lalanne, J.-P. Hugonin, and Q. Cao, Use of grating theories in integrated optics, J. Opt. Soc. Am. A **18**, 2865–2875 (2001).

[60] Q. Cao, Ph. Lalanne, and J.-P. Hugonin, Stable and efficient Bloch-mode computational method for one-dimensional grating waveguides, J. Opt. Soc. Am. A **19**, 335–338 (2002).

[61] R. Pregla and W. Pascher, The method of lines, in: Numerical Techniques for Microwave and Millimeter Waves Passive Structures, edited by T. Itoh (J. Wiley Publishers, New York, 1989), pp. 381–446.

[62] S. Helfert and R. Pregla, Efficient analysis of periodic structures, J. Lightwave Technol. **16**, 1694–1702 (1998).

[63] P. Russell, Photonic crystal fibers, Science **299**, 358–362 (2003).

[64] J. C. Knight, T. A. Birks, P. S. J. Russell, and D. M. Atkin, All-silica single-mode optical fiber with photonic crystal cladding, Opt. Lett. **21**, 1547–1549 (1996).

[65] R. F. Cregan, B. J. Mangan, J. C. Knight, T. A. Birks, P. S. J. Russell, P. J. Roberts, and D. C. Allan, Single-mode photonic bandgap guidance of light in air, Science **285**, 1537–1539 (1999).

[66] H. A. Bethe, Theory of diffraction by small holes, Phys. Rev. **66**, 163–182 (1944).

[67] C. J. Bouwkamp, On Bethe's theory of diffraction by small holes, Philips Res. Rep. **5**, 321–332 (1950).

[68] R. Sambles, More than transparent, Nature **391**, 641 (1998).

[69] M. M. J. Treacy, Dynamical diffraction in metallic optical gratings, Appl. Phys. Lett. **75**, 606–608 (1999).

[70] Q. Cao and Ph. Lalanne, Negative role of surface plasmons in the transmission of metallic gratings with very narrow slits, Phys. Rev. Lett. **88**, 057403 (2002).

[71] U. Schröter and D. Heitmann, Surface-plasmon-enhanced transmission through metallic gratings, Phys. Rev. B **58**, 15419–15421 (1998).

[72] J. A. Porto, F. J. García-Vidal, and J. B. Pendry, Transmission resonances on metallic gratings with very narrow slits, Phys. Rev. Lett. **83**, 2845–2848 (1999).

[73] Y. Xie, A. Zakharian, J. Moloney, and M. Mansuripur, Transmission of light through slit apertures in metallic films, Opt. Exp. **13**, 4485–4491 (2005).

[74] D. Pacifici, H. J. Lezec, H. A. Atwater, and J. Weiner, Quantitative determination of optical transmission through subwavelength slit arrays in Ag films: Role of surface wave interference and local coupling between adjacent slits, Phys. Rev. B **77**, 115411 (2008).

[75] H. Lezec and T. Thio, Diffracted evanescent wave model for enhanced and suppressed optical transmission through subwavelength hole arrays, Opt. Exp. **12**, 3629–3651 (2004).

[76] A. G. Borisov, F. J. G. Abajo, and S. V. Shabanov, Role of electromagnetic trapped modes in extraordinary transmission in nanostructured materials, Phys. Rev. B **71**, 075408 (2005).

[77] D. Crouse and P. Keshavareddy, Polarization independent enhanced optical transmission in one-dimensional gratings and device applications, Opt. Exp. **15**, 1415–1427 (2007)

[78] M. H. Lu, X. K. Liu, L. Feng, J. Li, C. P. Huang, Y. F. Chen, Y. Y. Zhu, S. N. Zhu, and N. B. Ming, Extraordinary acoustic transmission through a 1D grating with very narrow apertures, Phys. Rev. Lett. **99**, 174301 (2007).

[79] M. M. J. Treacy, Dynamical diffraction explanation of the anomalous transmission of light through metallic gratings, Phys. Rev. B **66**, 195105 (2002).

[80] Ph. Lalanne, C. Sauvan, J. C. Rodier, and J.-P. Hugonin, Perturbative approach for surface plasmon effects on flat interfaces periodically corrugated by subwavelength apertures, Phys. Rev. B **68**, 125404 (2003).

[81] Z. Sun, Y. S. Jung, and H. K. Kim, Role of surface plasmons in the optical interaction in metallic gratings with narrow slits, Appl. Phys. Lett. **83**, 3021–3023 (2003).

[82] G. Gay, O. Alloschery, B. V. Lesegno, C. ODwyer, J. Weiner, and H. J. Lezec, The optical response of nanostructured surfaces and the composite diffracted evanescent wave model, Nature Phys. **2**, 262–267 (2006).

[83] G. Gay, O. Alloschery, B. V. Lesegno, J. Weiner, and H. J. Lezec, Surface wave generation and propagation on metallic subwavelength structures measured by far-field interferometry, Phys. Rev. Lett. **96**, 213901 (2006).

[84] M. Mansuripur, A. R. Zakharian, and J. V. Moloney, Transmission of light through small elliptical apertures, Opt. Photon. News **15**, 44–48 (2004).

[85] M. Sarrazin and J.-P. Vigneron, Light transmission assisted by Brewster-Zennek modes in chromium films carrying a subwavelength hole array, Phys. Rev. B **71**, 075404 (2005).

[86] Z.-Y. Li, I. E. Kady, K.-M. Ho, S. Y. Lin, and J. G. Fleming, Photonic bandgap effect in layer-by-layer metallic photonic crystals, J. Appl. Phys. **93**, 38–42 (2003).

[87] F. Marquier, K. Joulain, and J.-J. Greffet, Resonant infrared transmission through SiC films, Opt. Lett. **29**, 2178–2180 (2004).

[88] P. Lalanne and J.-P. Hugonin, Interaction between optical nano-objects at metallo-dielectric interfaces, Nature Phys. **2**, 551–556 (2006).

[89] P. Lalanne, J. C. Rodier, and J.-P. Hugonin, Surface plasmons of metallic surfaces perforated by nanohole arrays, J. Opt. A, Pure Appl. Opt **7**, 422–426 (2005).

[90] N. Garcia and M. Nieto-Vesperinas, Theory of electromagnetic wave transmission through metallic gratings of subwavelength slits, J. Opt. A, Pure Appl. Opt. **9**, 490–495 (2007).

[91] Ph. Lalanne and G. M. Morris, Highly improved convergence of the coupled-wave method for TM polarization, J. Opt. Soc. Am. A **13**, 779–784 (1996).

[92] M. G. Moharam, E. B. Grann, D. A. Pommet, and T. K. Gaylord, Formulation for stable and efficient implementation of the rigorous coupled-wave analysis of binary gratings, J. Opt. Soc. Am. A **12**, 1068–1076 (1995).

[93] J. B. Pendry, Negative refraction makes a perfect lens, Phys. Rev. Lett. **85**, 3966–3969 (2000).

[94] N. Fang, H. Lee, C. Sun, and X. Zhang, Sub-diffraction-limited optical imaging with a silver superlens, Science **308**, 534–537 (2005).

[95] L. Kipp, M. Skibowski, R. L. Johnson, R. Berndt, R. Adelung, S. Harm, and R. Seemann, Sharper images by focusing soft X-rays with photon sieves, Nature **414**, 184–188 (2001).

[96] Q. Cao and J. Jahns, Focusing analysis of the pinhole photon sieve: individual far-field model, J. Opt. Soc. Am. A **19**, 2387–2393 (2002).

[97] Q. Cao and J. Jahns, Nonparaxial model for the focusing of high-numerical-aperture photon sieves, J. Opt. Soc. Am. A **20**, 1005–1012 (2003).

[98] Q. Cao and J. Jahns, Modified Fresnel zone plates that produce sharp Gaussian focal spots, J. Opt. Soc. Am. A **20**, 1576–1581 (2003).

[99] Q. Cao and J. Jahns, Comprehensive focusing analysis of various Fresnel zone plates, J. Opt. Soc. Am. A **21**, 561–571 (2004).

[100] W. Chao, B. H. Harteneck, J. A. Liddle, E. H. Anderson, and D. T. Attwood, Soft X-ray microscopy at a spatial resolution better than 15 nm, Nature **435**, 1210–1213 (2005).

[101] G. Schmahl, D. Rudolph, P. Guttmann, and O. Christ, Zone plates for X-ray microscopy, in: X-Ray Microscopy, Vol. 43, edited by G. Schmahl and D. Rudolph (Springer-Verlag, Berlin, 1984), pp. 63–74.

[102] E. H. Anderson, V. Boegli, and L. P. Muray, Electron beam lithography digital pattern generator and electronics for generalized curvilinear structures, J. Vac. Sci. Technol. B **13**, 2529–2534 (1995).

[103] E. H. Anderson, D. L. Olynick, B. Harteneck, E. Veklerov, G. Denbeaux, W. Chao, A. Lucero, L. Johnson, and D. Attwood, Nanofabrication and diffractive optics for high resolution X-ray applications, J. Vac. Sci. Technol. B **18**, 2970–2975 (2000).

[104] R. Menon, D. Gil, G. Barbastathis, H. I. Smith, Photon-sieve lithography, J. Opt. Soc. Am. A **22**, 342–345 (2005).

[105] G. Vaschenko, A. G. Etxarri, C. S. Menoni, J. J. Rocca, O. Hemberg, S. Bloom, W. Chao, E. H. Anderson, D. T. Attwood, Y. Lu, and B. Parkinson, Nanometer-scale ablation with a table-top soft X-ray laser, Opt. Lett. **31**, 3615–3617 (2006).

[106] V. Domingo, B. Fleck, and A. I. Poland, The SOHO mission: An overview, Solar Phys. **162**, 1–37 (2004).

[107] J. L. Soret, Über die durch Kreisgitter erzeugten Diffractionsphänomene (in German), Ann. Phys. Chem. **156**, 99–113 (1875).

[108] G. Andersen, Large optical photon sieve, Opt. Lett. **30**, 2976–2978 (2005).

[109] D. G. Grier, A revolution in optical manipulation, Nature **424**, 21–27 (2003).

[110] V. Daria, J. Glückstad, P. C. Mogensen, R. L. Eriksen, and S. Sinzinger, Implementing the generalized phase-contrast method in a planar-integrated micro-optics platform, Opt. Lett. **27**, 945–947 (2002).

[111] N. B. Simpson, K. Dholakia, L. Allen, and M. J. Padgett, The mechanical equivalence of the spin and orbital angular momentum of light: an optical spanner, Opt. Lett. **22**, 52–54 (1997).

[112] G. Biener, Y. Gorodetski, A. Niv, V. Kleiner, and E. Hasman, Manipulation of polarization-dependent multi-vortices with quasi-periodic subwavelength structures, Opt. Lett. **31**, 1594–1596 (2006).

[113] K. Iga, Y. Kokubun, and M. Oikawa, Fundamentals of Microoptics – Distributed-index, Microlens, and Stacked Planar Optics (Academic Press, Tokyo, 1984).

[114] R. Gomez-Reino, M. V. Perez, and C. Bao, Gradient-index optics – fundamentals and applications (Springer, Berlin, 2002).

[115] R. Gomez-Reino, M. V. Perez, C. Bao, and M. T. Flores-Arias, Design of GRIN optical components for coupling and interconnects, to be published in Laser Photonics Rev. (2008).